University of Groningen

Bachelor Thesis

An analysis of the chemical abundances in halo star g18-39

About the origin and composition of a high proper motion star.

rijksuniversiteit groningen

Author:
Alessandro Angrilli Muglia

Supervisor:
Prof. Dr. E. Tolstoy
Second Examiner:
Dr. E. Starkenburg

Abstract

The origin of high proper motion stars in the Milky Way is object of long standing interest in astronomy. In this thesis, we analyse a high resolution UVES spectrum of g18-39, a high proper motion star associated with the halo. This star is of interest because it is a solar-analog star, but presents very different characteristics than our Sun from a kinematic point of view. The analysis was carried out using iSpec, a spectral analysis tool, to search for and where possible measure the abundance of r-process chemical elements, specifically Europium, Thorium and Uranium. We measured the abundances of these elements using equivalent width analysis where possible, otherwise comparing our spectrum with synthesised spectra. We found a higher than solar metallicity for Europium, while a sub-solar metallicity for Thorium and Uranium. Finally, we explained our results associating the origin of g18-39 to the Gaia-Enceladus merger event.

Contents

1 Introduction

To paraphrase the roman philosopher Lucius Annaeus Seneca: what a beautiful thing is the human mind, it cannot understand itself, yet it tries to understand the whole universe around it! In his Naturales Quaestiones, the philosopher attempted to answer questions about meteorology, physics, and astronomy. Since then, scientists have made a lot of progress, yet the thirst for knowledge has not diminished. Nowadays, the questions we pose ourselves in astronomy are not about the shape of our planet, or whether or not it is the center of the Universe. Today, we know the Earth is revolving around the Sun, which in turn is revolving around the center of the Milky Way, our galaxy.

To try and dig deeper into the Universe we have built more and more powerful machinery throughout the years. Thanks to the concept of open archives, it is possible for us to use the spectrum measured from the UVES, the Ultraviolet and Visual Echelle Spectrograph, many years ago by other researchers. This instrument belongs to ESO (European Southern Observatory), an intergovernmental association supported by 16 Member States. The instrument is one of the most advanced high resolution spectrographs in the world and is a component of the Very Large Telescope, situated in the high altitude desert of Atacama, in Chile. Its technology, in combination with perfect geographical positioning is what makes the data of such a high quality.

Figure 1: *Image of the inside of the Very Large Telescope, where the UVES instrumentation is situated.*

In this thesis we study a star in our Galaxy, the star g18-39. We analyse the UVES spectrum of this object, and in doing so, we will try to answer some questions: what is the chemical composition of this star? Can we see any heavy elements such as Europium, Thorium or Uranium?

Based on the elements we found and other characteristics, can we determine the origin of g18-39? Is it possible to infer that this star has originated in the halo of the Milky Way? And if not, where could it possibly come from?

The reason why we chose this specific star is because, as we will see in the upcoming sections, g18-39 is a Solar-analog star, which however presents some peculiar characteristics. In the catalogue by Cayrel de Strobel et al., 1997 Solar-analogue stars are defined as having the following properties:

- Temperature similar to the one of the Sun ($\pm$ 500K).
- On the Zero Age Main Sequence it needs to be within 1 magnitude of the Sun (so it has to be burning hydrogen in its core).
- No close companion: the star shoulld not be in a binary system, or more bodies orbiting around each other.

By studying a star with these similarities to the Sun, which has been widely studied in literature, we can compare their spectra, their motion and other important characteristics. The analysis will help us discover all the similarities, and the differences between the two, helping us answer the questions that we have just posed. Trying to find an answer to them will help us not only to understand the origin of the Milky Way, but also has general consequences for our understanding of the origin and interactions of Milky Way-like galaxies in the Universe.

The outline of the thesis is as follows: first we will give some background information about what stellar spectra are, and how we can use them in our analysis. Then, we will give some background information useful to understand the results and discussion, where we will try to answer the questions. Finally, we will discuss improvements to our approach and analysis and draw conclusions.

2 Stellar Spectra

Stellar spectra allow us to determine the physical properties of a star such as surface temperature (T_{eff}), pressure (log(g)), abundances of many chemical elements (Z), as well as radial velocity (V_r). To determine these properties of star g18-39, we analyse its spectrum taken from archival ESO/UVES observations. Before jumping into the analysis, however, we will describe the relevant theoretical background needed to understand the approach taken and the results.

2.1 Chemical abundances of individual elements

Studying the abundance of chemical elements in a star means to find the relative number of atoms/ions of an element, compared to another one in the photosphere of the star. Abundances are usually given in units of dex (decimal exponential), according to the formula:

$$[X/Y] = log\left(\frac{N_X}{N_Y}\right)_* - log\left(\frac{N_X}{N_Y}\right)_\odot \tag{1}$$

where N_X and N_Y are the atoms per unit volume of elements X and Y. The fraction between the two is corrected relative to the ratio of these two same elements in the Sun (Hinkel et al., 2014). A common abundance is the [Fe/H]: iron constitutes the final product of exothermic nuclear fusions in a stellar core and is released primarily in SN Ia explosion, while hydrogen is the most common element. Iron has the largest number of individual spectral lines in the stellar spectrum of Sun-like stars.

Abundances of elements are generally presented relative to iron ([X/Fe]). Studying this ratio can give us information about what has happened in past stellar formation. By comparing the elemental abundances of g18-39 with the latest data about stellar populations originated in-situ in the Milky Way (Belokurov and Kravtsov, 2022), we can infer the origin of our star, because stars share the properties of the environment in which they formed. More about this can be found in section 5.

For a better understanding of the reader we will also define the metallicity of a star. The term metallicity is used to indicate the abundance of elements heavier than helium. We specify this since in our analysis we might use the terms abundance and metallicity interchangeably.

2.2 Continuum and Absorption lines

If there existed a perfect black-body, it would emit radiation as a continuum following Planck's law:

$$B_\nu(T) = \frac{2h\nu^3}{c^2}\frac{1}{e^{h\nu/kT} - 1}. \tag{2}$$

Although close, stars are not perfect emitters, and as it can be seen in Figure 2 the spectrum of a star typically differs noticeably from a Planck's spectrum.

One reason the spectrum of a star is not only a black-body-like continuum is because of opacity effects. Electromagnetic radiation generated inside of a star interacts with atoms present in the atmosphere on its way out, often exciting or ionising them. This can affect the shape of the continuum and spectral lines in several different ways. The depth of selected lines is the main tool we use to analyse the properties of a star. The flux of a line does not drop only at an exact wavelength, but it can spread to a wider range of wavelengths. That is because each

line undergoes three different types of broadening: natural, Doppler (or thermal), and pressure (Leblanc, 2010). These effects need to be disentangled from each other. The width of a line depends also on the abundance of the element in question.

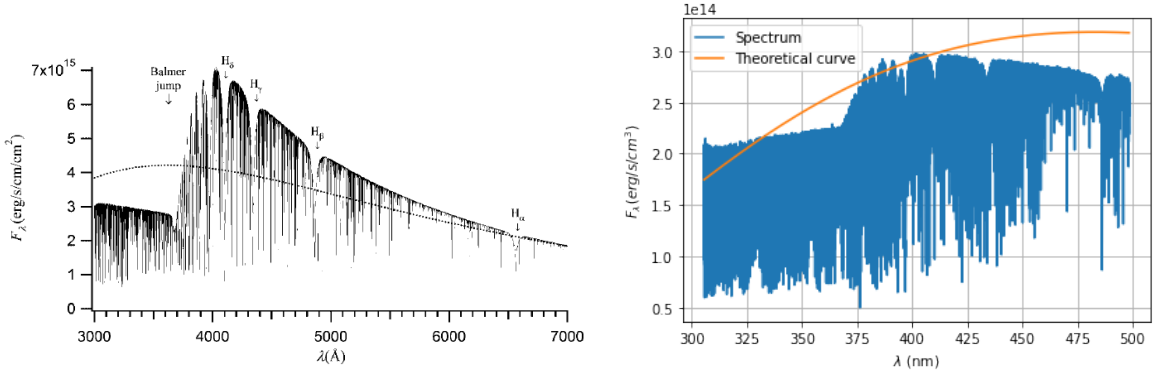

Figure 2: *On the left the spectrum of an A-type star (T_{eff} = 8000K) simulated using the Phoenix stellar atmosphere code by Allard et al., 2000, compared with a perfect black-body spectrum with T=8000K (Leblanc, 2010). On the right, the UVES spectrum of g18-39, a G0 star, retrieved from ESO archive (Dekker et al., 2000 compared with a black-body spectrum with T=6000K. This temperature was chosen because of the value of T_{eff} presented in the paper by Nissen and Schuster, 2010.*

To study in detail the shape of an absorption line, we use the standard concept of equivalent width (W_λ). W_λ is defined as a hypothetical ideal line with a rectangular profile, which makes the flux drop to 0 at the center (see Figure 3) and has the same integrated flux deficit from the continuum as the line itself (Stahler and Palla, 2004). The equivalent width can be written as:

$$W_\lambda = \int \frac{F_c - F_\lambda}{F_c} d\lambda = \int \left[1 - \frac{F_\lambda}{F_c}\right] d\lambda \tag{3}$$

From which we can conclude that the equivalent width depends both on the flux of the line, and on the value of flux of the continuum. In some cases we calculated abundances using equivalent widths, thus it is important to accurately determine the continuum level of a spectrum. How to do so will be explained in detail in the analysis section.

After one finds the continuum, it can be used to normalise the spectrum in order to make accurate abundance analysis possible. As stated earlier, a black-body differs from a continuum, but not only because of effects into the star itself. Other effects disturbing the continuum are instrumental effects: spectrographs have different efficiencies at different wavelengths. In Figure 2 we can compare the spectrum of a simulation (left) and its relatively smooth curve, with the spectrum of our star (right) which has an instrumental signature. These effects can be reduced when a continuum is being fitted.

Before determining if a chemical element is present or not in a star, it is important to reduce instrumental effects as much as possible. The elements we are looking for tend to have weak absorption lines, and are barely visible, so it is relatively easy to confuse them with noise and continuum uncertainties. Moreover, an added effect that might make the analysis more challenging is line blending. This phenomenon occurs when two absorption lines are so close to be

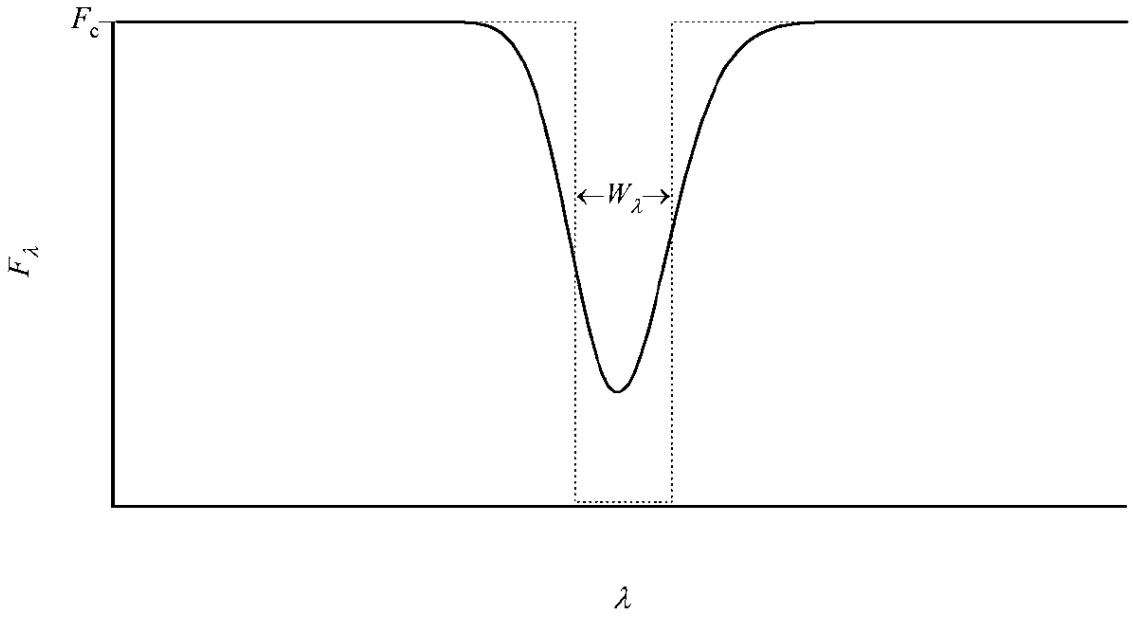

Figure 3: *The area subtended by the absorption line with respect to the continuum is the same as the area of the rectangle that has equivalent width W_λ (Leblanc, 2010).*

blended and appear as one. Such outcome could be due to one of the aforementioned broadening effects, or because of a not high enough resolution of the spectrum.

In a spectrum in general the larger the equivalent width, the more absorbing atoms or ions of an element are present and the position of each line corresponds to one of the energy states of this element. Heavier elements attract strongly their electrons, requiring high energy photons to strip them from their nucleus. That is the reason why transitions of elements with $Z > 30$ happen in the blue, at approximately $\lambda < 430nm$ or less (Hansen, 2022), and it is also the reason why we decided to analyse the blue wavelength range ($< 500nm$).

2.2.1 Balmer lines

One more important and noticeable discontinuity when looking at blue spectra is the so-called Balmer jump. This feature is not present in all stars, but it can be observed in B-type to G-type stars, so from Figure 2 we can see that g18-39 is within this range. In conjunction with the Balmer jump, we can find very strong hydrogen absorption lines, also known as the Balmer lines. These lines are generated when hydrogen absorbs radiation at the atomic level n=2 and based on the width of these lines it is possible to determine the effective temperature of a stellar atmosphere. For this work, they create problems to accurately measure weak absorption lines in the same wavelength range.

2.2.2 r-process

While elements lighter than Fe can be produced in the interior of a star, for heavier elements a different process is needed. One of the fundamental ways of producing approximately half of

the heaviest elements is the rapid neutron-capture process, or r-process (Holmbeck et al., 2018). There are multiple events in which the r-process can occur. For stars in the early history of the Milky Way, it is possible that the r-process enhancement might have occurred due to SNe Type II, or possibly because of kilonovae explosions, mergers of two neutron stars (Sumiyoshi, 2002, Holmbeck et al., 2018, Roederer et al., 2018). Stars with a high level of r-process formed elements are usually referred to as r-II stars, and often Europium is used as a probe for r-process enrichment (Roederer et al., 2018).

Tolstoy et al., 2009 infer that a major plausible candidate for r-process formation is SNe Type II. If a star would be enriched by SNe, it would need to undergo one or multiple events in its surroundings to reach the level of enrichment of a kilonova. As argued by Yamazaki et al., 2021, however, it is not possible for core collapsing supernovae to reach the energy level leading to the formation of the heaviest elements in elevated abundances. On the other hand, a neutron star merger event might have enough energy to start high r-process element formation. In Roederer et al., 2018 they focus on the phenomenon of the kilonova since it might have led to the formation of most of the heavy elements we observe and their derivation can be explained with a progenitor of $10^3 \sim 10^4 M_\odot$.

2.3 Kinematics

Every star in the sky is moving. The most commonly used frame of reference in astronomy defines the dimensions of movement as: proper motion right ascension (μ_α) and proper motion declination (μ_δ), the two components in the plane of the sky, and radial velocity (V_r), which is the velocity along the line of sight (see Figure 4). g18-39 is catalogued to be a high proper motion star (SIMBAD, n.d.), which means a star with a significant movement across the sky compared to the other stars. According to Gaia, 2020 DR3 data, the star moves at 301.1309 mas/yr. Such a high movement comes from the fact that, unlike most of the other stars, g18-39 is moving at an angle to the Galactic disk. We are able to observe this star with such precision as it is currently crossing the disk in the solar neighbourhood.

From Gaia, 2020 DR3 we also retrieved an estimate of the radial velocity, which was found to be -234.0163 km/s. We compared it with the value proposed by Nissen and Schuster, 2010 of -234.1 km/s, in order to have an estimate of what we can expect from our data analysis. As shown in Figure 4 the radial velocities are appointed with two different colours depending on the direction. That is because when a star is moving away along the line of sight it will be redshifted. Contrarily, when the radial velocity has a negative value, the star we are observing it is coming towards us and will be blueshifted. g18-39 is thus blueshifted.

For spectral analysis it is important to account for redshift (or blueshift). Its radial velocity shifts the positions of spectral lines, thus we expect the center of each line to be moved by a few nanometers to the left of the their theoretical position. For g18-39 it will be fundamental in the analysis to correct for blueshift to correctly identify the absorption lines in the spectrum.

Finally, when a galaxy is being formed, because of conservation of angular momentum, all the stars forming around the center will be rotating around it in the same direction. These stars are defined to be "prograde", while stars completing revolutions in the opposite direction are defined to be "retrograde". The angular momentum usually has the bodies rotating in the same plane as well. This is the reason why we can identify stars in the Galactic disk very easily. We

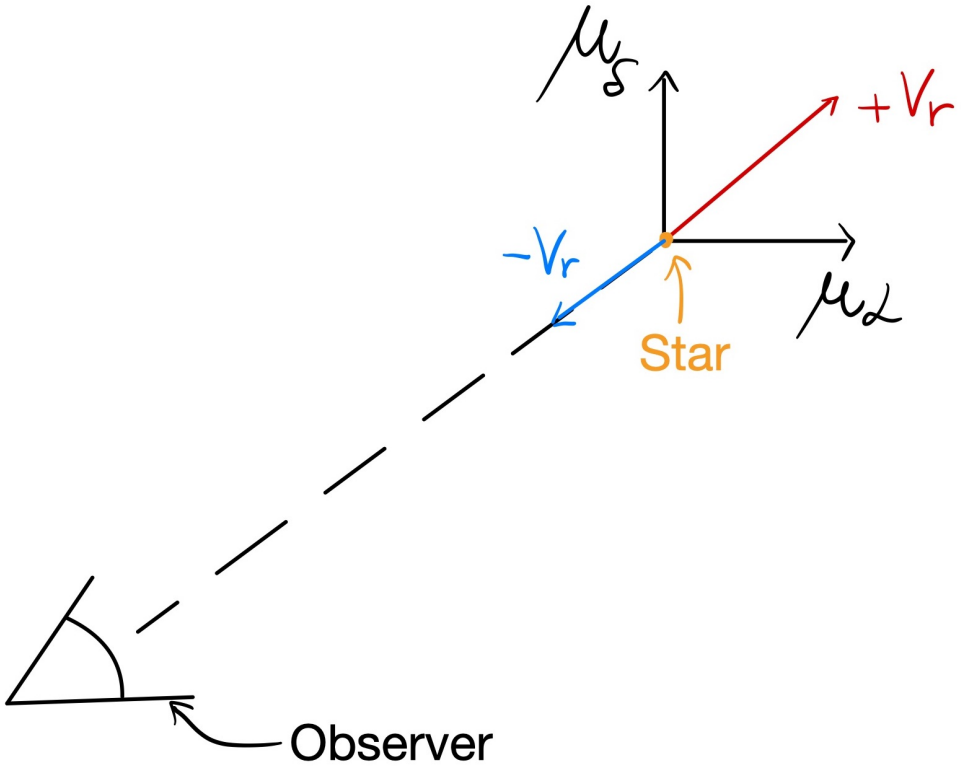

Figure 4: *A scheme of the velocities from an observer's point of view.*

will talk more in depth about the Galaxy in section 3.

2.4 Spectral synthesis

Another important tool for the study of abundances is the synthetic spectral fitting technique. Thanks to computer based modelling and given the atmospheric parameters of a star, we are able to study abundances in a spectrum by synthesising one. If we are looking for a specific abundance, the computer will generate a range of different spectra, each one corresponding to a pre-computed grid of abundances of that element (Blanco-Cuaresma et al., 2014). For each of these spectra, a χ^2 test is run. When the synthetic spectrum matches the actual data with its best fit, the computer will provide the elemental abundance coming from the best matching synthetic spectrum. This technique can also be used for normalisation. Assuming known atmospheric parameters, it is possible to synthesise a continuum that then can be used to normalise the spectrum.

Such technique is not only used for a general synthesis of a spectrum. The computing power of a machine can be exploited to synthesise regions around a single absorption line. As we explained in the previous sections, an absorption line can be found at a specific wavelength. One can create multiple synthetic spectra varying the abundance of the corresponding element and check the behaviour of the line as a consequence. Similarly to a full spectrum, a spectral line can be synthesised around known data, or it can be used to make models of abundances.

2.5 iSpec

iSpec is a software dedicated to the analysis of stellar spectra[1], developed by Blanco-Cuaresma et al., 2014, Blanco-Cuaresma, 2019. There are two ways of using the platform. The first one is to directly download the python routines and run them, and the second one is to use the graphic user interface provided. The first approach has a much wider potential with what one can do with a spectrum, but is much more time consuming to learn, so, due to time constraints, we proceeded using the iSpec interface, which still allowed us to compute all the operations needed.

The iSpec module is designed for the user to determine atmospheric parameters and chemical abundances for AFGKM stars. It is possible to choose from two different atmosphere models to work with, and we decided to go with the more modern one, namely Gustafsson et al., 2008. Moreover, it was possible to choose between several radial transfer codes, for which we decided to use Gray, 2021.

iSpec is a user friendly platform that can automatically perform a number of otherwise complex operations, which we will hereby explain:

- Calculation of radial velocity and determination of resolution:

Using a spectral library, iSpec is able to determine the shift of spectral lines from their theoretical rest frame. In doing so, the system can also calculate an approximate value for resolution. In general, resolution is defined as the power of an instrument to observe (or resolve) features in a spectrum. The resolving power of the instrument for a certain spectrum is generally calculated according to the formula:

$$R = \frac{\lambda}{\Delta\lambda} \tag{4}$$

However, when resolution is not provided, iSpec uses a different method to estimate it. When finding the radial velocity, iSpec calculates the estimation with the formula:

$$R = \frac{c}{FWHM_{line} - FWHM_{theoretical}} \tag{5}$$

where c is the speed of light and FWHM stands for Full Width Half Maximum of an absorption line. The method is not only used in the iSpec interface but is also used in current research studies such as the one by Berg et al., 2022. As also reported in the manual[2], this method is not as precise as obtaining value for resolution directly from literature. The spectrum of g18-39 is a medium resolution UVES spectrum (R∼33000).

- Determination of signal-to-noise ratio (S/N) from errors:

Another important parameter affecting the quality of observations is the signal-to-noise ratio (S/N). This represents the intensity of the signal of a feature one is interested in, divided by the noise in the same region. This value is useful to determine how good an observation is. In fact, the higher this value, the more accurate any measurement will be. For a more precise and accurate analysis, one has to aim for the best resolution and S/N possible. iSpec is capable of estimating S/N by dividing each flux measurement by its relative error and taking the mean of all the values.

[1] iSpec homepage:https://www.blancocuaresma.com/s/iSpec
[2] iSpec manual: https://www.blancocuaresma.com/s/iSpec/manual/usage/resolution

- Continuum determination and normalisation of the spectrum:

There are four alternative models to calculate the continuum on the interface. The one we will use because we deem the most accurate is the splines method. This operation consists in dividing the spectral range in N amount of splines and fitting a polynomial through each of these, with a degree between 1 and 5. The system is able to automatically find strong lines and they will be avoided as much as possible. Moreover, one can use the error of each measurement as the weight for the fitting process. After having fitted the continuum it is possible to normalise the spectrum with a simple operation that consists in dividing the whole spectrum by the just determined curve.

- Fitting absorption lines:

In order to find absorption lines, iSpec lets the user choose from several atomic line lists. Based on the chosen line list, the software matches absorption lines in the spectrum to the ones on the list.

- Parameter and abundance determination using equivalent widths:

Based on the equivalent widths of fitted lines, iSpec is able to both estimate atmospheric parameters (T_{eff}, log(g), etc...), as well as give the abundance of a specific element (only one at a time). The abundances are provided both in comparison to hydrogen and iron.

- Parameter and abundance determination with synthesis:

Taken the spectrum of a star, one can select certain segments, and iSpec will synthesise different stellar spectra varying the atmospheric parameters and abundances of a selected element. For each synthesis, a χ^2 test is done to determine the goodness of fit. When one of the synthesised spectra reaches an optimal fit, the system returns a value of the metallicity of the element one had selected. This method is an alternative to equivalent widths. Nevertheless, there is a limit: iSpec's graphical interface is only able to perform this operation for elements up until praseodymium.

- Synthesise full spectrum:

Inputting atmospheric parameters iSpec can synthesise a spectrum as explained in section 2.4.

3 The Milky Way

Our own Galaxy, where the Solar System is situated, is called the Milky Way, because of its bright white colour painted along the starry night. Humankind has been viewing our Galaxy since the dawn of time, but we discovered only in the 1920s what precisely we are looking at and that it is not alone, but it is just one out of the many galaxies out there. The Milky Way is considered to be a "benchmark" galaxy, meaning it shares common features with many other spiral galaxies, and a deep study of it should give insights about the history, formation and future of numerous galaxies in the universe. Moreover, we are in a privileged position for the study of our Galaxy since we live in the middle of it.

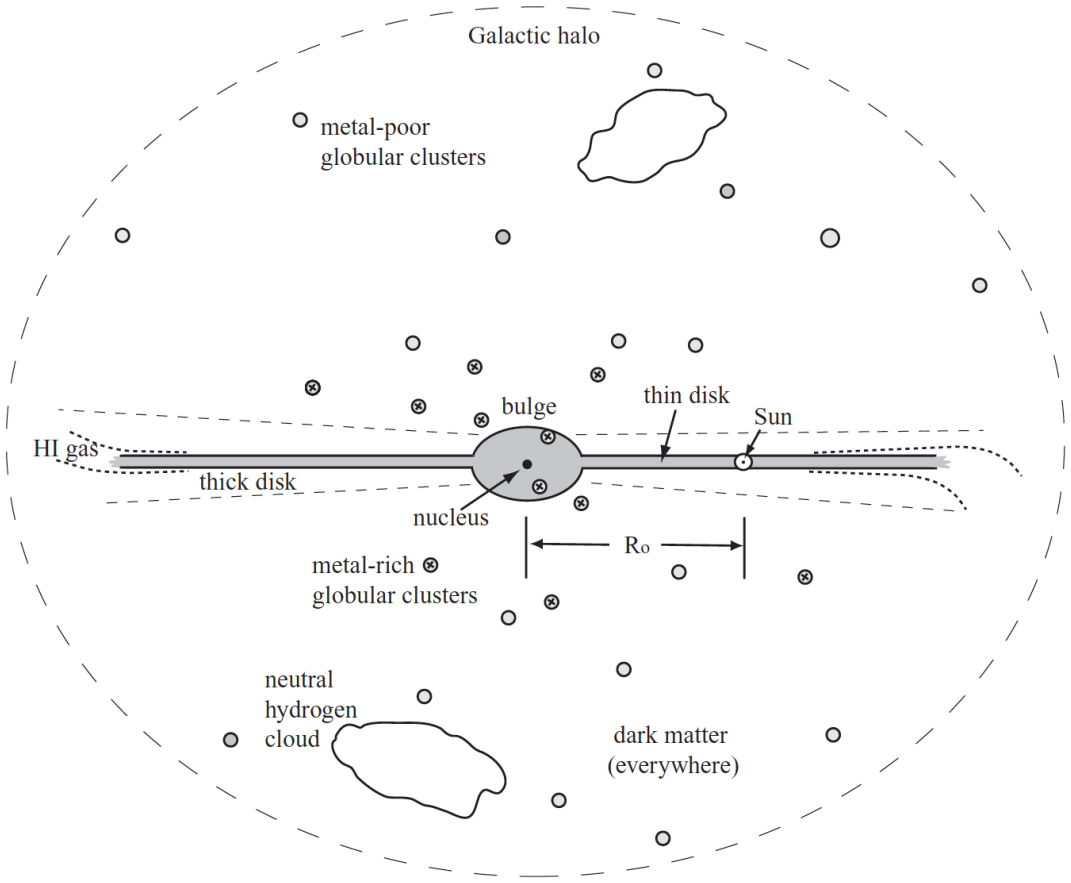

Figure 5: *An illustration of the most important components of the Milky Way (Sparke and Gallagher, 2010).*

A schematic view of the Milky Way is given in Figure 5. At the center we can find a supermassive black hole, imaged for the first time in the current year by Akiyama et al., 2022! Around it we can find a bulge, from which along the Galactic plane extends the the thin disk, which contains the spiral arms. The thick disk surrounds its thin counterpart. Going outwards we can find neutral hydrogen clouds, as well as various globular clusters and dwarf galaxies orbiting the Milky Way. Finally, the whole Galaxy is surrounded by the Galactic halo, which encloses the just listed components plus dark matter. The halo and its components are the ones we are most interested in and that we will discuss in the upcoming sections.

3.1 Galactic Halo

The halo is defined as a spheroidal region surrounding the Milky Way. There are three main components that define this region: the stellar, gaseous and dark matter halos (Bland-Hawthorn and Gerhard, 2016). The gaseous halo is a cloud of hot diffuse gas. It includes a "high metallicity" part ($Z \geq 0.3Z_{\odot}$, meaning [Fe/H] $\geq$ -0.57) exponentially decaying, which has a scale length of a few kpc, and a much more diffuse part with lower metallicity (Yao and Wang, 2007). The dark matter halo is being observed indirectly: it is being studied through proxies such as the kinematics of halo stars, or the kinematics satellite dwarf galaxies and clusters affected by the total mass of the Milky Way plus dark matter.

The stellar halo comprises around 1% of the whole stellar population of the Milky Way, and is formed by a population of old, high proper motion, metal poor stars, amongst which we can find g18-39. As stated by Cooper et al., 2010, the stellar halo is not formed by a single population, but is a superposition of many components. Studying the chemical abundances of g18-39 and comparing with the chemical composition of the stellar halo is useful to determine the local origin of this star. In case the comparison does not show similar characteristics, it would then be interesting to see where g18-39 would have formed.

The current most credited theory about the formation of our Galaxy states Milky Way's thick disk and its inner halo have been formed due to mergers including the one with Gaia-Enceladus (Helmi et al., 2018), as well as smaller building blocks (Massari et al., 2019) These results pose the doubt about the existence of an "in situ" halo. We hope that the analysis conducted in this paper might constitute a small contribution to providing information about to solve the mystery of the origin of the Milky Way in more detail.

3.2 Dwarf Galaxies orbiting the Milky Way

A dwarf galaxy is a gathering of stars gravitationally bound stars of size up to $\sim 1/10$ of the size of the Milky Way. There is not a clear boundary to define the difference in stellar mass between a dwarf galaxy and a globular cluster. Typically the distinction between the two is made by defining dwarf galaxies to contain dark matter, while the globular clusters do not. However, the definition is not to be taken as an absolute: other studies (i.e. Brown et al., 2019) have claimed a component of dark matter in ω Cen.

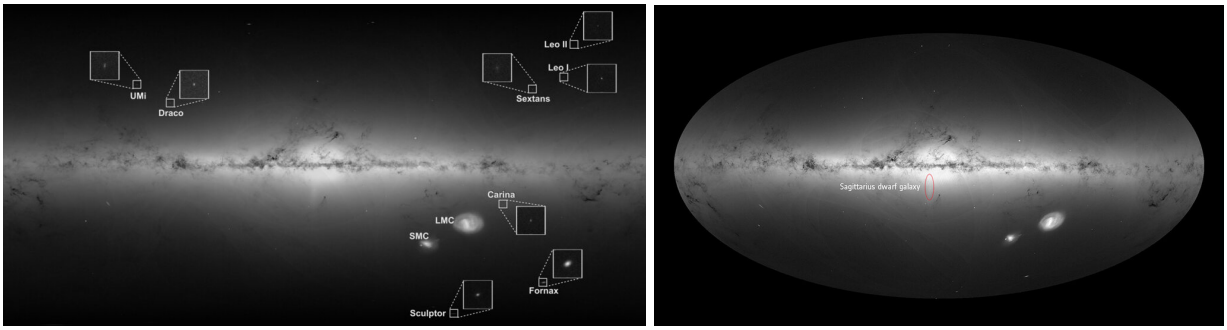

Figure 6: *The major satellite galaxies of the Milky Way are represented on the left (ESA, 2022). These dwarf galaxies feel the gravitational pull of our galaxy, but are still separate from it. Contrarily, the right image shows the Sagittarius dwarf galaxy, already absorbed by its progenitor. The image is an illustration from the study by Antoja et al., 2018.*

In studies by Yang et al., 2022 it has been shown how dwarf galaxies orbiting the Milky Way develop stellar streams due to the tidal interactions between the two. We can compare the findings by Yang et al., 2022 with the stellar trails shapes found by Ibata et al., 2019 or by Wang et al., 2022. From the comparison, we can argue how the current trails of ω Cen or the Sagittarius dwarf galaxy are a flash-forward of what the Fornax galaxy will go through. If to this we add that the Gaia-Enceladus dwarf galaxy had an estimated mass of $\sim 6 \times 10^8 M_\odot$ (the approximate size of the Small Magellanic Cloud, Helmi et al., 2018), we see the evidence that the Milky Way is a result of multiple mergers of dwarf galaxies.

3.3 α element abundances

Stars enrich their surrounding interstellar medium at the end of their lives. The elements cast out by a star range from lighter elements to heavier ones depending on the star and the dispersal mechanism. We are particularly interested in nuclei belonging to the iron peak (Fe, Cr, Co, Ni, Cu, Mn) which are generated in SNe Ia, while α elements (C, O, Ne, Mg, Si, S, Ar, Ca), are so called because they originate in α processes, and form predominantly in type II SNe (Gebek and Matthee, 2022).

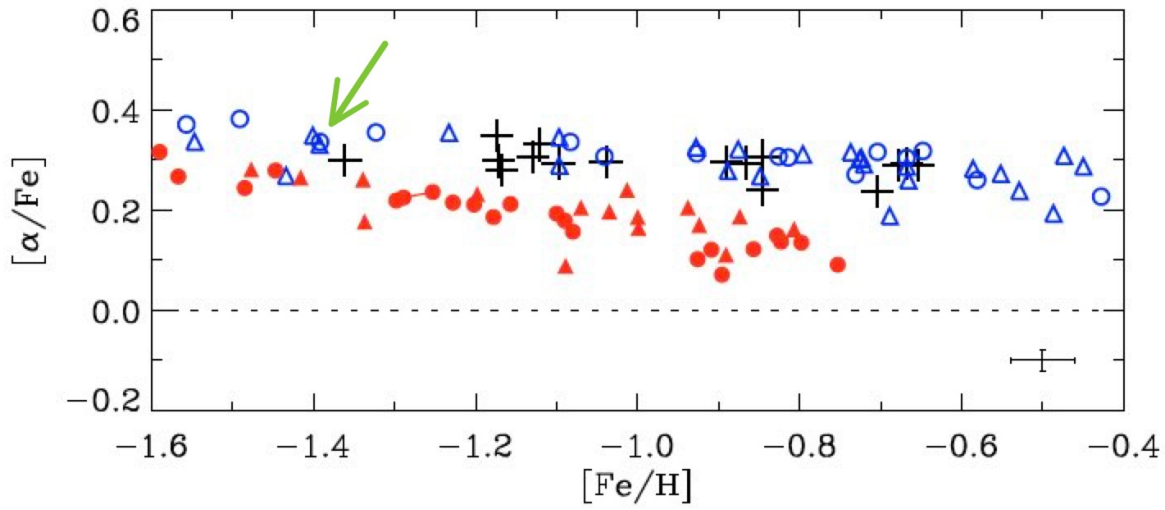

Figure 7: *Plot of [α/Fe] vs [Fe/H] for a sample of halo stars from Nissen and Schuster, 2010. The red symbols are low-α stars, the blue ones are high-α stars, and the crosses are thick disk stars. g18-39 is the open blue circle indicated by the green arrow.*

The α to iron abundance ratio [α/Fe] is an important indicator of the origin of a star, since the two different types of supernovae that affect this ratio have very different timescales. Thus α-abundance helps to reconstruct the history of star formation. In fact, the elements that enrich a star represent the footprint of the events happening in its neighbourhood before it was formed. In the paper by Hawkins et al., 2015, stars with low iron abundances ([Fe/H] $\leq$ -1.2) and low-α enhancement are considered to be formed outside of the Milky Way, and accreted in the halo later in their lifetime. Contrarily, if a star has a high-α a star could have been formed in situ. In their extensive study of high proper motion stars Nissen and Schuster, 2010 plotted various halo stars with high-α vs low-α, where we also found our star (see Figure 7).

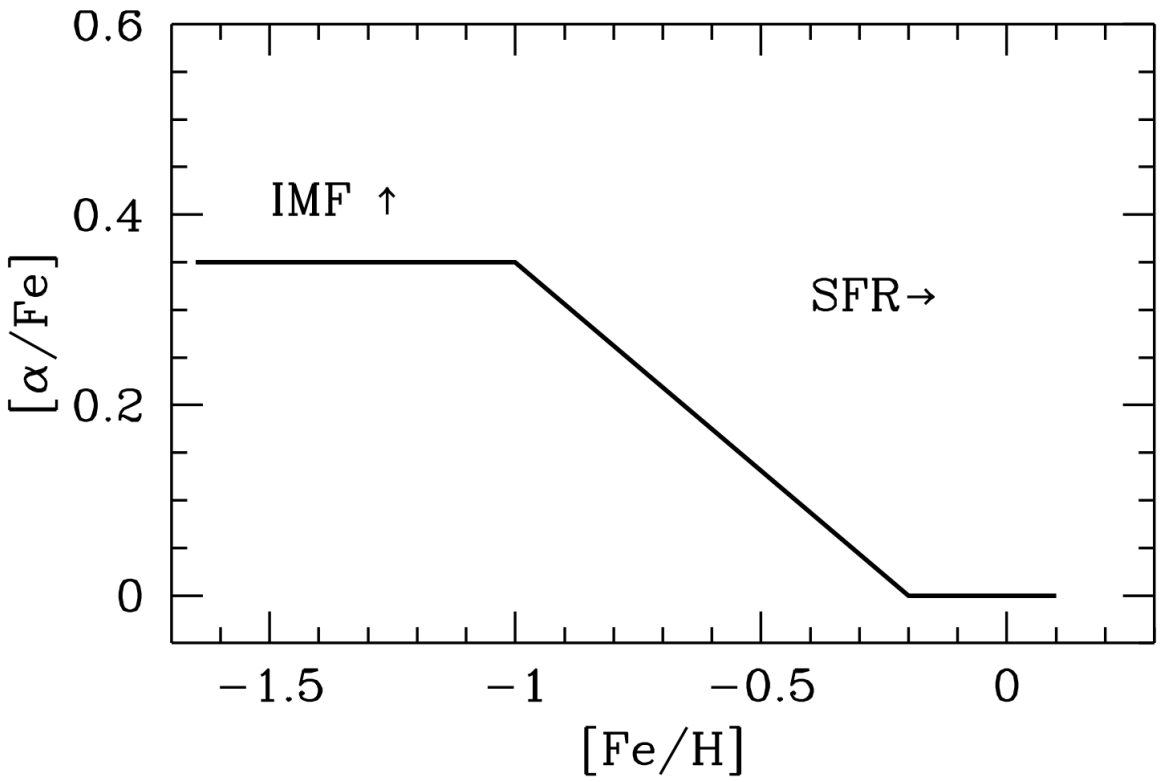

Figure 8: *Trend of [α/Fe] with metallicity [Fe/H]. Varying Initial Mass Function (IMF) could move the trend vertically, while a variation in the Star Formation Rate (SFR) could cause the function to move horizontally (From: McWilliam, 1997).*

In Figure 8 from McWilliam, 1997 we can see the relation between [α/Fe] and [Fe/H]. The knee we observe at around [Fe/H] = -1 is due to the onset of the first SNe type Ia. The function [α/Fe] vs [Fe/H] depends on the Initial Mass Function (IMF) of a star population, since stars with higher masses can produce more metals, thus enriching more the interstellar medium when becoming SNe. The Star Formation Rate (SFR) could also interest the position of the function. When more stars are forming, the gas is enriched of [Fe/H] at a faster pace before the first SN Type Ia occurs. Thus the knee (and the ankle) will move at higher values of [Fe/H].

3.4 g18-39

The word planet derives from the ancient Egyptian *planasthai*, which means "to wander". Since then, astronomers have made huge steps forward, and thanks to the newest technologies we know planets are not the only ones "wandering" around the sky, although of course much less rapidly than the planets of the Solar System. g18-39 belongs to a comoving group recently studied by Silva et al., 2012, and is named G18-39. The group was found to contain 25 so-called "moderately high proper motion stars". In the same paper, Silva et al., 2012 argue that these stars are contained in a velocity structure similar to that of a dwarf galaxy accreting onto the Milky Way, or following trails like ω Cen. The result is then comparable to the aforementioned results by

Ibata et al., 2019 and Wang et al., 2022, which also found stellar trails in their papers.

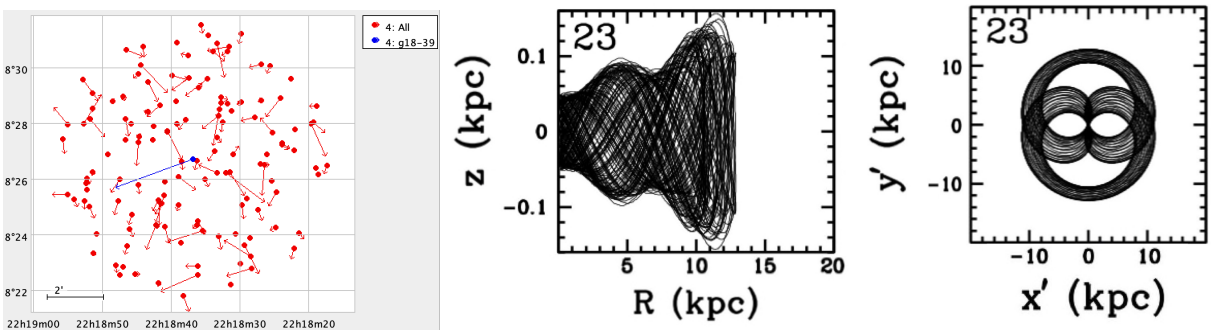

Figure 9: *On the left, the scaled proper motion of g18-39 compared to its neighbours within 5 arcseconds, visualised using TOPCAT and retrieving data from Gaia, 2020. In the middle, Schuster et al., 2018 plotted meridional orbits of stars of the group G18-39. Our star, g18-39, is the star number 23 in the paper, and we show its orbit here. On the right, the corresponding projected orbit on the Galactic plane, in the non-inertial frame of the Milky Way bar.*

As it can be seen in Figure 9, g18-39 has a much higher proper motion compared to all its neighbours. A deeper analysis about high proper motion stars of the G18-39 group was also made by Schuster et al., 2018, where they reconstructed the orbit of our star. The motion delineated by g18-39 does not follow the path of the $\approx 95\%$ of stars present in the thin disk: its motion seems to follow a pattern of precession of orbital path. Furthermore, in their analysis of halo stars, Nissen and Schuster, 2010 study velocities of these stars compared to thick disk stars motions. We reported the graph in Figure 10, where we can see that g18-39 is moving in a retrograde fashion.

More precisely the orbits of the stars in G18-39 has been described by Schuster et al., 2018 as resonating due to the Galactic bar, which would explain the anomalous motion of g18-39, enforcing the idea of the in-situ origin. However, we will be testing this hypothesis with our analysis. As mentioned in the introduction, g18-39 is a sun-like star, so we would expect its composition to be relatively similar to the one of our Sun, or at least share some common features. We first compare the calculated abundances and values for T_{eff} and log(g) with the ones measured by Nissen and Schuster, 2010, reported in Table 1.

ID	S/N	V_r (km/s)	T_{eff} (K)	log(g)	[Fe/H]	Class (low or high α)
g18-39	480	-234.1	6040	4.21	-1.39	high-α
[Na/Fe]	[Mg/Fe]	[Si/Fe]	[Ca/Fe]	[Ti/Fe]	[Cr/Fe]	[Ni/Fe]
-0.06	0.35	0.29	0.39	0.31	-0.01	-0.05

Table 1: *The table contains relevant parameters of the star in the first row, and calculated metallicities of various elements on the second row (from Nissen and Schuster, 2010).*

Some additional information about g18-39: in the paper by Nissen and Schuster, 2012 we can find a calculation of the mass $M_* = 0.8 M_\odot$ and a ratio of heavy-element mass of $Z = 0.0014$. Moreover, from Schuster et al., 2012 we also know the age of our star to be 11.4±1.0 Gyr. Age has been determined by plotting isochrones in the log(g) vs log(T_{eff}) plane, interpolating

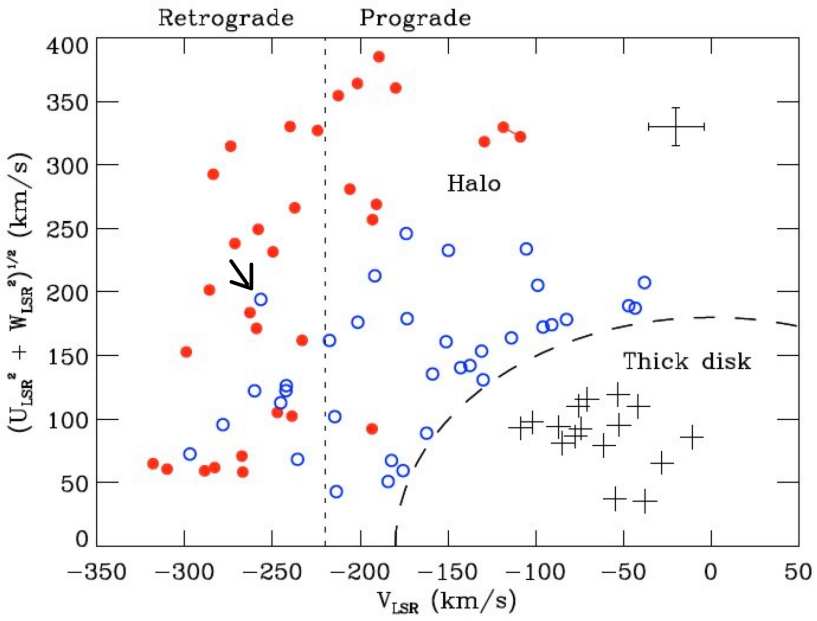

Figure 10: *The graph has again been retrieved by Nissen and Schuster, 2010. Hence the adopted convention is the same as the one in Figure 7. We have individuated g18-39 in this plot: the blue circle indicated by the arrow. It can be seen how the star falls in the subset of the retrograde high proper motion.*

exact spectroscopic values between these isochrones, and when the [α/Fe] and the [Fe/H] values corresponded to the ones of our star, the age of that particular isochrone was taken.

4 Analysing stellar spectra

The aim of this analysis is to investigate the spectrum of g18-39, to verify the presence of any heavy elements. We will focus particularly on Europium, Thorium and Uranium. As we will see, letting the machine determine the presence of these elements can be tricky, for this reason we will also check these lines by eye.

The analysis will proceed in the following way: we will develop a method to process data. This method will be tested on a set of test stars, and then we will apply such method to the UVES spectrum of g18-39. Finally, we will move on to analyse the processed data of our spectrum in search of the aforementioned elements.

4.1 Method

The method we have developed can be summarised with the steps in Figure 11.

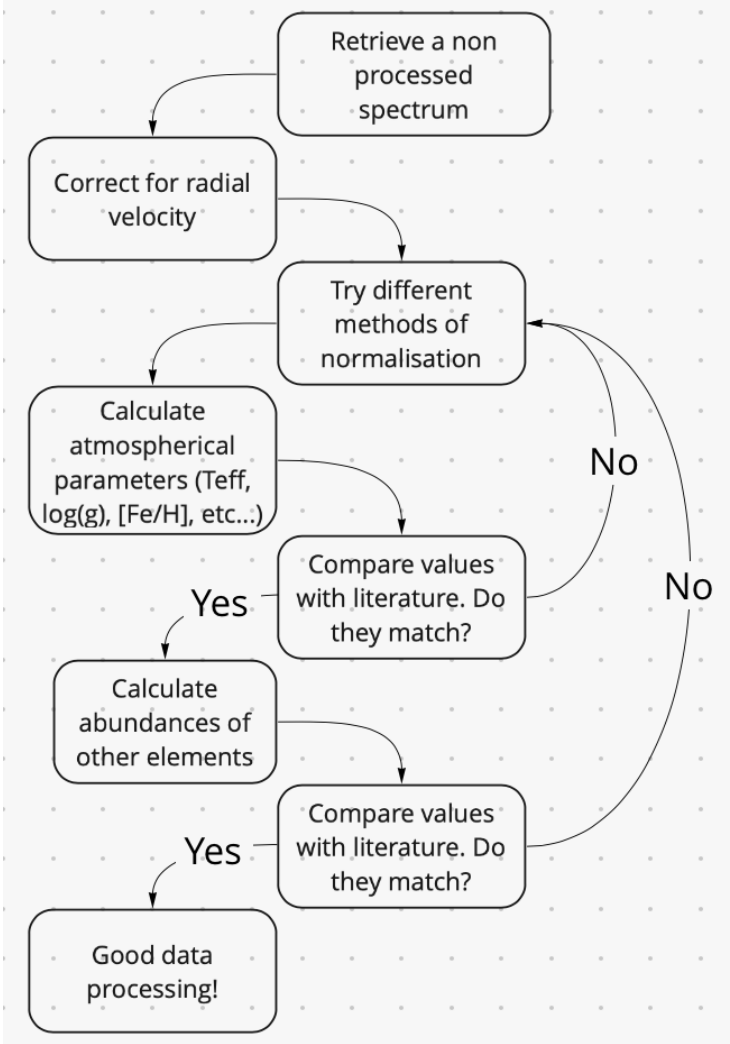

Figure 11: *Operations done summarised in a simple scheme.*

After having retrieved a non processed spectrum, we have to make sure that each atomic

line is at the correct wavelength. Thus we apply a correction to radial velocity, which can be calculated and corrected automatically in the system.

The next step is to fit a continuum with splines. We usually use a polynomial of degree 3 or 5 in this method. The reason why we choose the polynomial to be an odd number is because even functions are symmetric, thus they follow less easily the irregularities of spectra.

Having fitted the continuum, we can divide the spectrum by this curve. The next step is to fit iron lines to determine [Fe/H] abundance. From the equivalent widths of these absorption lines it is also possible to calculate atmospheric parameters. These values can be compared with literature, and if they were reasonable within a certain range, we would have proceeded to the next step. Otherwise, we would have started the normalisation process. We considered a normalisation to be accurate enough when the effective temperature was within ±50K, log(g) within ±0.3, and [Fe/H] in the boundary ±0.05 dex.

If the various atmospheric parameters fell within the ranges we just described, we would move on to fit absorption lines of other elements. We would calculate abundances with equivalent widths again, and compare these values with literature. If also these values were within the ±0.05 dex limit, or their error range included the literature value, we would have considered the normalisation method effective.

4.2 Benchmark stars

Benchmark stars are a set of common calibration stars. They are selected from various regions of the HR diagram, span a large range of metallicities, and their spectra have a high resolution and S/N ratio (Blanco-Cuaresma et al., 2014). These last two values allow elevated precision in the analysis of a spectrum, which is why benchmark stars are good to develop a consistent and reliable method.

We particularly selected some of them which have similar characteristics to the Sun, and thus g18-39 as well. The stars we analysed are: ESPaDOnS_HD49933-1, HARPS.GBOG_HD122563, HARPS.GBOG_psiPhe, ARVAL_Gmb1830, UVES_HD140283-1. We presented these stars as catalogued in the iSpec dedicated page for benchmarks[3].

We proceed to exemplify the case of the normalisation of ESPaDOnS_HD49933-1. In Figure 12 we present a comparison of the data we retrieved with the normalisation already carried out by Blanco-Cuaresma et al., 2014.

We corrected for radial velocity, fit a continuum and normalise the spectrum using splines. Then, in a range of 200 nm we could find approximately 1100 lines of Fe I and Fe II, limiting the depth from 5% to 100% compared to the continuum. Using the equivalent width of these lines we checked atmospheric parameters and [Fe/H] abundance.

In Figure 13 we show a comparison of a normalisation that yields parameters not consistent with the values proposed by Blanco-Cuaresma et al., 2014 versus an acceptable normalisation. In the image, we particularly focus on the feature of the Hβ line. The advantage of working with

[3] https://www.blancocuaresma.com/s/benchmarkstars

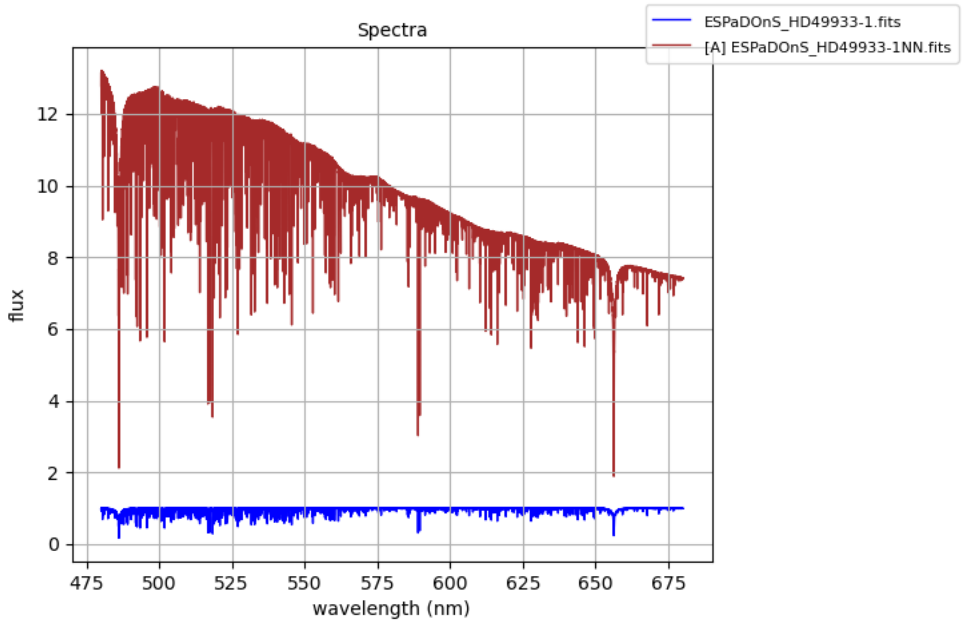

Figure 12: *An example of unprocessed data (red line) plotted with the spectrum already normalised by Blanco-Cuaresma et al., 2014 (blue line). The spectrum belongs to the star HD49933.*

benchmark stars is that we can check our results not only by checking abundances, but also by inspecting features visually.

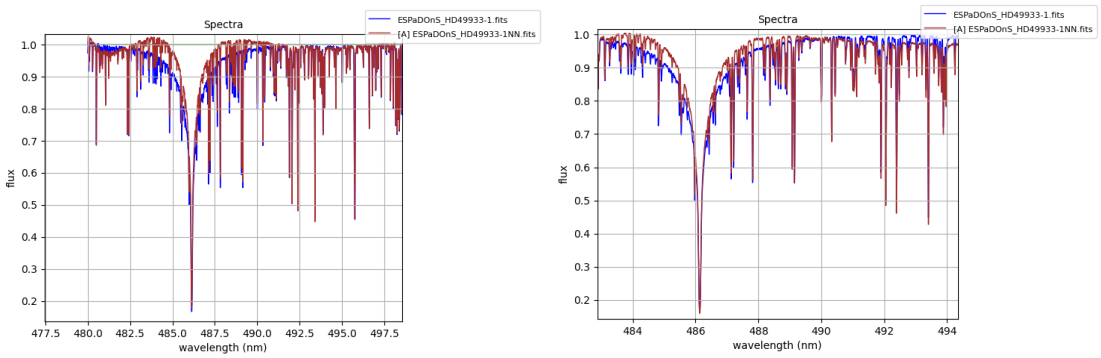

Figure 13: *In blue the spectrum normalised by Blanco-Cuaresma et al., 2014. In red the normalisation carried out by us. In the left image, we can see a normalisation which is considered a bad fit, while on the right is shown a good fit instead.*

In the iSpec dedicated page for benchmarks[4] it was possible to retrieve metallicities for Titanium and Nickel as well. For this reason, we compared those metallicities with the ones in the normalised spectrum in the right image of Figure 13. They were indeed within the ±0.05 dex limit, so we deemed our normalisation good enough.

In order to increase the precision of abundance determination, we decided to take an extra step: making a synthesis of the spectrum. Such technique constitutes an advantage since the

[4] https://www.blancocuaresma.com/s/benchmarkstars

abundance determination can reach high levels of accuracy with a relatively low error. The synthesis of the spectrum of HD49933 is presented in Figure 14.

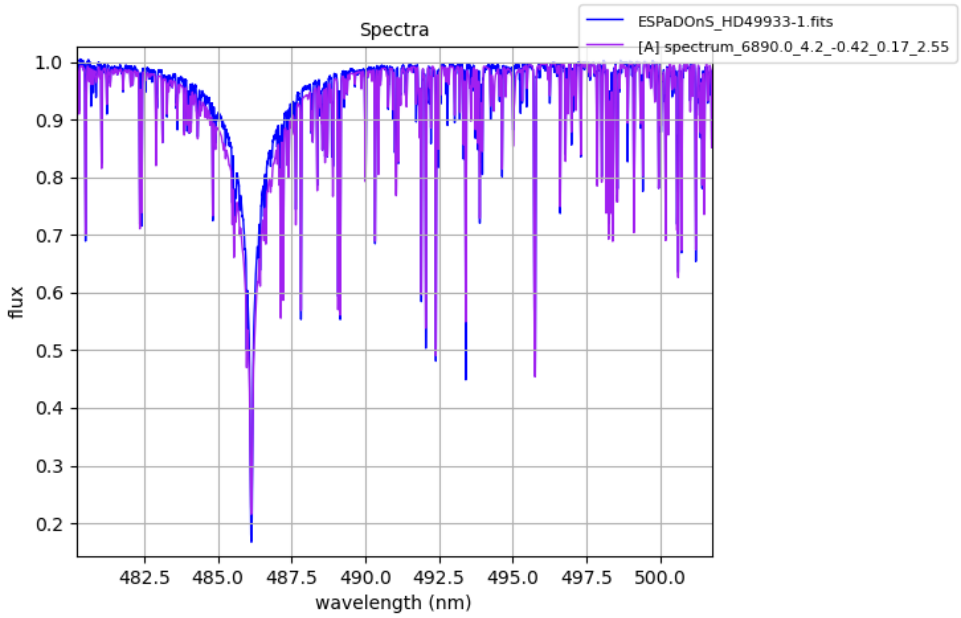

Figure 14: *The purple spectrum is a synthesis produced with the calculated atmospheric values. Features such as the Hβ and iron lines are coinciding, but smaller ones still different.*

After having completed the synthesis we checked values for Nickel and Titanium and they both fell within the ±0.02 dex range. The synthesis could be a powerful tool to compare the normalisation of the spectrum of g18-39.

4.3 g18-39

The subject of this study is the star g18-39. In this subsection we will describe the data that we retrieved. Then we will present our values for calculated atmospheric parameters and abundances. Finally, we will examine absorption lines of Europium, Thorium and Uranium.

4.3.1 Data

The spectrum we retrieved from the UVES database is presented in Figure 15. It ranges from a wavelength of 305.545nm to 498.399nm. It has an integrated exposure time of 1333.0012s and it has been taken the 2003-08-19 at 07:16 (Program ID 71.B-0529).

We repeated the steps described in section 4.1, and we also created a synthesis to measure abundances with increased accuracy. For this star Nissen and Schuster, 2010 had calculated metallicities for multiple elements, so it was possible to perform a more detailed comparison. We report the results in Table 2.

As it can be seen, comparing this table with Table 1, most of the values are within a small margin of each other, and all of them fall within the error. It needs to be noted that for α enhancement Nissen and Schuster, 2010 do not provide a value, but classify the star as "high-α".

ID	S/N	V_r (km/s)	T_{eff}(K)	log(g)	[Fe/H]	[α/Fe]
g18-39	72.26	-234.06	6064	4.41	-1.41 ± 0.05	0.30 ± 0.03
[Na/Fe]	[Mg/Fe]	[Si/Fe]	[Ca/Fe]	[Ti/Fe]	[Cr/Fe]	[Ni/Fe]
-0.05 ± 0.78	0.53 ± 0.27	0.27 ± 0.73	0.25 ± 0.45	0.27 ± 0.13	0.02 ±0.67	-0.04 ± 0.43

Table 2: *A table containing results of the found metallicities.*

However, we can compare our result with Figure 7 to confirm the obtained value. A difference that stands out to the eye is the discrepancy in the S/N, but as pointed out in the iSpec manual[5] it is more accurate to simply use the literature value.

As stated before, these metallicities were obtained thanks to the use of both equivalent widths and a synthesis. In Figure 15 how the synthesis agrees with the data when measuring relatively strong lines from lighter elements. Nevertheless, iSpec is not able to adapt the synthesis for each element, especially the heavier ones. The code is only able to reproduce the main features with high accuracy. For this reason, we decided to proceed only with the normalised spectrum.

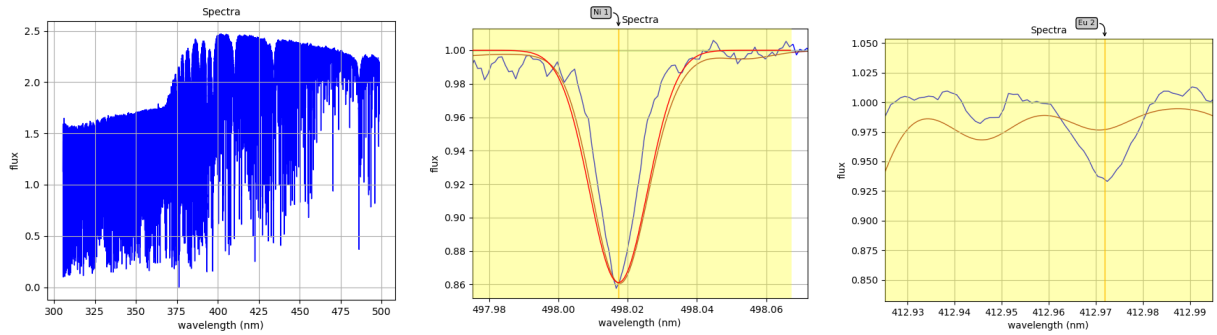

Figure 15: *On the left the UVES spectrum of g18-39 as retrieved from the database of ESO (Dekker et al., 2000). In the middle an image of the synthesis (red) agreeing with the data (blue) on a Ni I at ∼498nm line. On the right, the data and the synthesis have a discrepancy around the the Eu II line at ∼413nm.*

4.3.2 Heavy element analysis

When our data processing was finally complete and deemed accurate, we moved on to the search of Europium, Thorium and Uranium.

The first element we searched for is Europium. Europium is the 63rd element of the periodic table. For the analysis of this element, we focus on Eu II, or ionised Europium, since at the T_{eff} of g18-39 it is hard to find the neutral atom. According to the paper by Hinkle et al., 2000, there are 6 absorption lines in the wavelength range of our spectrum, and we decided to analyse two of them. These lines were selected as they were visible in our spectrum.

[5] https://www.blancocuaresma.com/s/iSpec/manual/usage/flux_errors

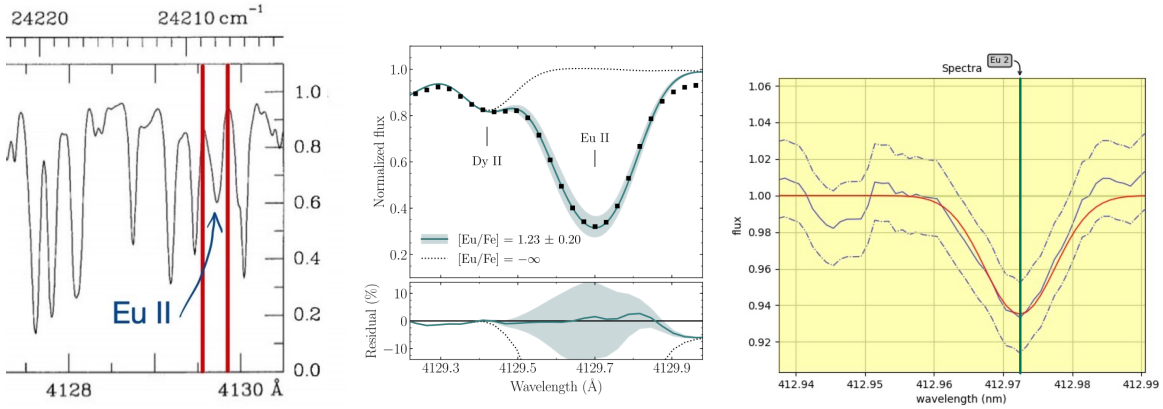

Figure 16: *A comparison between the Sun by Hinkle et al., 2000 (left), synthetic spectra of star 2MASS J09544277+5246414 by Holmbeck et al., 2018 (center), and our star (right) for the Eu II line at wavelength 412.973 nm indicated in green. In the spectrum of g18-39 the intensity of the line is less intense, but by looking at it we can infer that it definitely corresponds to a Europium line.*

The first absorption line we observed is the one at 412.973nm, presented in Figure 16. The absorption line was also automatically individuated by the system. For this reason, it was possible to calculate an abundance automatically. The value found was [Eu/Fe] = 0.44 dex. Since the star analysed by Holmbeck et al., 2018 is "the most actinide-enhanced r-II star yet discovered", we expect their metallicity to be an upper bound. The value we have found verifies this condition.

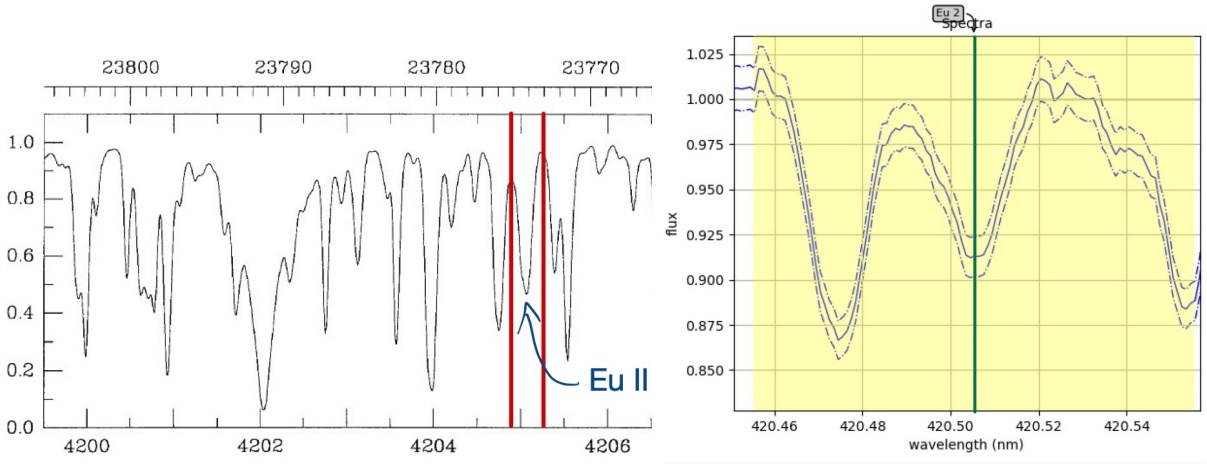

Figure 17: *A comparison between Sun by Hinkle et al., 2000 (left), and g18-39 (right) for the Eu II line at wavelength 420.505 nm.*

In Figure 17 we present a comparison of the absorption line at 420.505 nm. We can see that in our Figure the system was not able to fit a profile for the absorption line, due to the fact that this line is not present in any iSpec line list. Nevertheless, we think that it corresponds to an absorption line, similar to the one in Figure 16.

The next element we study is Thorium, of which the atomic number is 90. Being one of the heavies stable elements in nature, we expect its abundance to be relatively low.

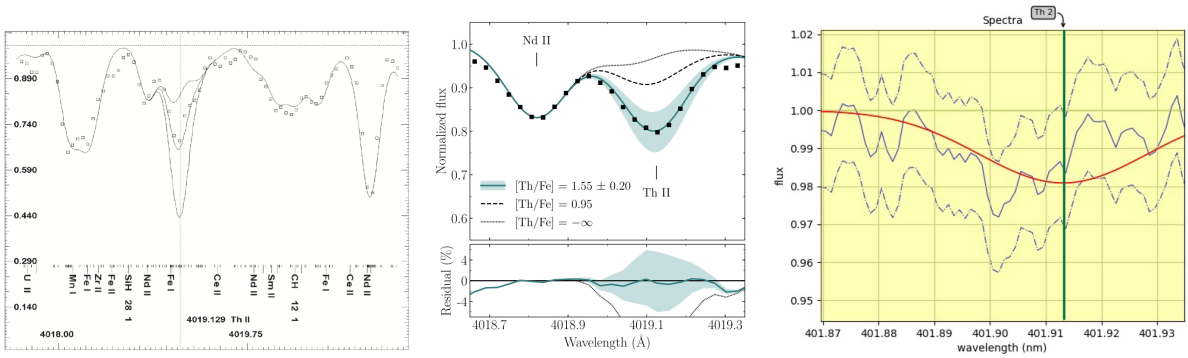

Figure 18: *A comparison between a synthesis of HD221170 by Yushchenko et al., 2005 (left), one by Holmbeck et al., 2018 (middle), and g18-39 (right) for the Th II line at wavelength 401.913 nm. In the analysis on the left are plotted three different syntheses, one with -1.18 dex and a deviation of* ± 0.5.

In Figure 18 we present two syntheses that focus on the presence of Thorium. The pattern followed by the spectrum of g18-39 is similar to the line at -1.23 dex in Yushchenko et al., 2005. As we can see in both graphs, the line is blended with the iron line at $\lambda \sim 419.01nm$. However, the system finds the line, but poorly fits a line mask to it. For this reason, we will simply conclude that our spectrum has a thorium component, but more accurate methods are needed to determine the abundance.

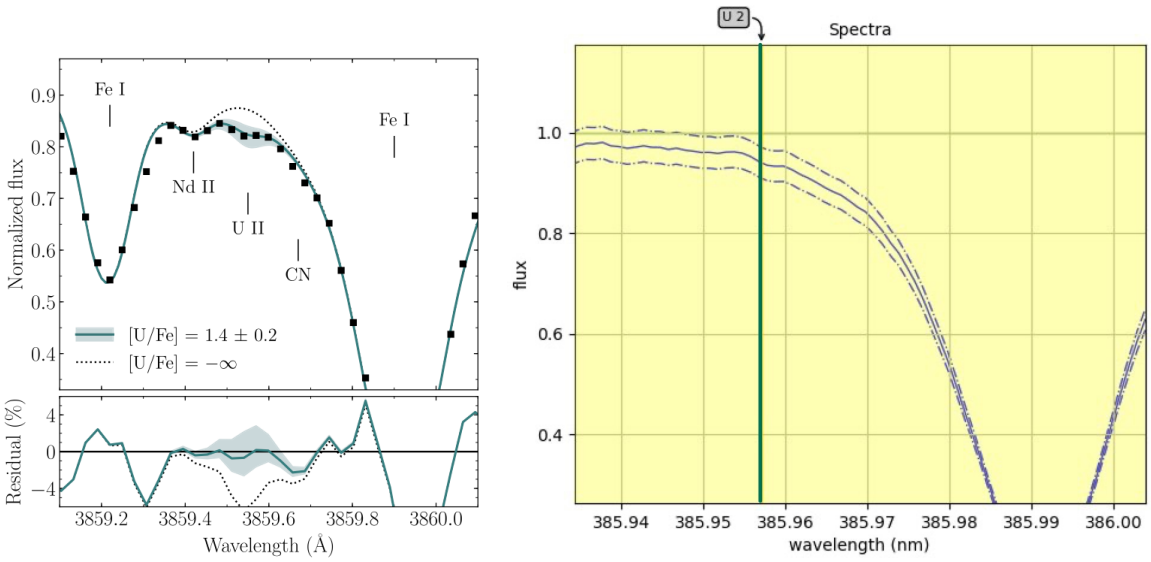

Figure 19: *A comparison between the star by Holmbeck et al., 2018 (left), and g18-39 (right) for the U II line at wavelength 385.957 nm.*

Finally, we moved on to the last element of our analysis, namely Uranium. Finding a line can be challenging, especially when we are trying to discern it from noise. We present our attempt at observing a line in Figure 19.

Now, is there any Uranium? In the spectrum of g18-39 there is a wobble in the continuum juxtaposed to the wavelength where one should see the line. It might be due to noise, but we think it is too coincidental to show a pattern so similar to the high metallicity star on the left Figure 19. If we were to compare the Neodymium line in the graph, we would not find it in the spectrum of g18-39. Nevertheless, we are also missing Neodymium features in Figure 18, comparing g18-39 to the spectrum by Holmbeck et al., 2018.

In conclusion, it would be possible to make an argument about the presence of Uranium. Nevertheless, the depth in the line observed by Holmbeck et al., 2018 is more than 5% from the continuum, while ours is barely 1%. Further research is needed to answer this question more precisely.

In the next section, we discuss these results in more detail, and we will try to answer the questions that we posed in the Introduction.

5 Discussion

In the previous section we looked into the possibility of observing heavy metals such as Europium, Thorium and Uranium. While for the first one is generally more simple to observe spectral lines, Thorium and Uranium are usually harder to find. We believe that in g18-39 we were able to find Europium in even higher amounts than the Sun.

Regarding the second element, Thorium, the only detectable line is in the proximity of much stronger iron lines. Due to the blending, one can hardly deduce the presence of this element. Nevertheless, we think that in Figure 18 the small feature of the normalised spectrum is similar to the result published by Yushchenko et al., 2005. However, in our analysis we also deduced that the metallicity of Thorium is [Th/Fe]<0. In order to be enriched by heavy elements, a star needs to have in its neighbourhood a relatively high amount of highly energetic events to enrich it with r-process formed elements. This means that before the origin of g18-39 other stars should have formed, lived and died to enrich its interstellar medium.

With its atomic number Z=92, Uranium is the heaviest stable nucleus in nature. Due to the incredibly high amount of neutron flux required to produce Thorium and Uranium, there is still a debate about the formation of this element (Sumiyoshi, 2002, Roederer et al., 2018). For this reason we did not expect to find excessive amounts of it in our star, and the observations confirmed this trend. From Figure 19 it is possible we detect a relatively low Uranium presence. Additionally, it is possible to argue that since Thorium has a low abundance, also Uranium must have. That is because if an event such as a supernova did not have enough energy to generate Thorium, it most likely will not be able to generate Uranium either.

In section 3.4 we talked about the heavy element abundances. With the results we obtained we believe that indeed g18-39 is a star that has been enhanced by r-process formed elements, but on the lighter end. Thus it can be argued that, in comparison to the Sun, the star g18-39 was in contact with an environment where more explosions happened, but they were less violent than the ones happening in the solar neighbourhood.

But then, did g18-39 originate in the halo or not?

One can argue that this star originated in a dwarf galaxy which has accreted the Milky Way. If we look at the abundance analysis we conducted, we can see that although g18-39 is a solar-analogue, it hardly follows the pattern of solar abundances for the elements that we have observed, suggesting an origin in a different environment like a dwarf galaxy.

Another reason why g18-39 might have seen its early days in a dwarf galaxy distinct from the Milky Way is because of its motion. Its irregular and retrograde orbit, and the orbit of the group G18-39 as a whole, appear to represent the trail of a merger that happened a long time ago. The reason why the merger must have happened in a relatively big time frame is that if it happened recently we might have recognised still G18-39 as a galaxy, or at least a globular cluster. That would also explain why trying to find a merger pattern is more challenging than in cases such as with ω Cen. The Milky Way might have undergone many mergers in the past, not just major mergers.

There are, however, some arguments that suggest g18-39 is an "in situ" halo star. The

unusual shape and retrograde direction of the orbit can be explained with an orbit that is resonating. Moreover, according to multiple studies (Hawkins et al., 2015, Schuler et al., 2021) if a star with [Fe/H] = -1.39 has also a high-α enhancement, then we expect it to have its origin in the Milky Way. As there are globular clusters originated and orbiting around the halo, it is possible that the group G18-39 is nothing but one of these bodies falling slowly into the Milky Way.

There is, finally, an explanation that lies somewhere in between the two aforementioned solutions. According to Schuler et al., 2021, all the stars in the G18-39 group cannot all be considered "members" of a group. However, all these resonating stars might be still an observable result of the Gaia-Enceladus merger. Based on what we have gathered, this solution is the one that seems the most reasonable to us. Nevertheless, there is still a lot of work to do to prove such a statement, and some questions that would come up: is there an "in-situ" halo? Was the halo that we observe today actually defined by the Gaia-Enceladus merger?

In conclusion, it is safe to say that this work does not answer all the questions asked initially with certainties. Instead it offers a new small perspective about the study of high proper motion stars, and might be a small piece to figure our the puzzle about the origin our galaxy.

6 Conclusion

In this thesis we analysed the spectrum of the star g18-39. We developed a method to normalise the spectrum, and then we made a synthesis of what we had, reaching similar values to atmospheric parameters and abundances found in literature. After establishing that the synthesis was not suitable for our purpose, we used our normalised spectrum to look for heavy elements, namely Europium, Thorium, and Uranium. We concluded that the first of these elements is present in our star in more-than-solar abundance, while we believe Thorium and Uranium to be present, but in sub-solar abundance.

Of these two last results, we did not have a value or a range of abundances to present with certainty given the weakness of the absorption lines. We think that this result could be achieved to a higher degree of precision of different syntheses varying the abundance of these elements were run. As we already mentioned previously, this is not possible to do via the graphical interface, only using python code. For a better comparison with Holmbeck et al., 2018 it would have also been interesting to investigate more in detail the abundance of Nd II.

Another point of improvement could be to observe more lines of both Uranium and Thorium. Being rare, these elements have faint lines, thus we would have to increase our chances of seeing a line. Furthermore, we compared our metallicity with a number of other stars in the Milky Way, whereas it would be interesting to compare our star with the average Milky Way metallicity, with other stars in the group G18-39, or with the metallicity of the Gaia-Enceladus merger.

At the end of our analysis, based on the results we had gathered, we went on to discuss the possible origin of our star, inferring it might be a remainder from the Gaia-Enceladus merger. In conclusion, further research not only in our star, but in halo stars is still needed to find definitive answers to questions such as the existence of an in-situ halo.

7 Acknowledgements

First of all, I would like to thank Prof. Dr. E. Tolstoy, this thesis would have not been possible without her. She dedicated me an incredible amount of time and had immense patience throughout the whole process. Most of all, I found her enthusiasm inspiring and it is what motivated me every day to try and do better. Thank you.

I want to take this opportunity to express my gratitude to Luigi Delle Donne, the first person to ever introduce me to the world of physics. From him, I learnt to love science and he was the first one outside of my family who believed in me. Thank you.

Last but not least, I would like to thank Giancarlo Giuliani. In the time I spent with him I learnt to pursue my passions no matter where they would take me. From him, I took inspiration to undertake the journey to become myself. Thank you.

References

Akiyama, K., Alberdi, A., Alef, W., Algaba, J. C., Anantua, R., Asada, K., Azulay, R., Bach, U., Baczko, A.-K., Ball, D., Baloković, M., Barrett, J., Bauböck, M., Benson, B. A., Bintley, D., Blackburn, L., Blundell, R., Bouman, K. L., Bower, G. C., ... Zeballos, M. (2022). First sagittarius a* event horizon telescope results. i. the shadow of the supermassive black hole in the center of the milky way. *The Astrophysical Journal Letters*, *930*, L12. https://doi.org/10.3847/2041-8213/ac6674

Allard, F., Hauschildt, P. H., & Schwenke, D. (2000). Tio and h₂o absorption lines in cool stellar atmospheres. *The Astrophysical Journal*, *540*, 1005–1015. https://doi.org/10.1086/309366

Antoja, T., Helmi, A., Romero-Gómez, M., Katz, D., Babusiaux, C., Drimmel, R., Evans, D. W., Figueras, F., Poggio, E., Reylé, C., Robin, A. C., Seabroke, G., & Soubiran, C. (2018). A dynamically young and perturbed milky way disk. *Nature*, *561*, 360–362. https://doi.org/10.1038/s41586-018-0510-7

Belokurov, V., & Kravtsov, A. (2022). From dawn till disc: Milky way's turbulent youth revealed by the apogee+gaia data. *Monthly Notices of the Royal Astronomical Society*, *514*, 689–714. https://doi.org/10.1093/mnras/stac1267

Berg, T. A. M., Cupani, G., Figueira, P., & Mehner, A. (2022). Performance of espresso's high-resolution 4 × 2 binning for characterising intervening absorbers towards faint quasars. *Astronomy Astrophysics*, *662*, A35. https://doi.org/10.1051/0004-6361/202243208

Blanco-Cuaresma, S., Soubiran, C., Heiter, U., & Jofré, P. (2014). Determining stellar atmospheric parameters and chemical abundances of fgk stars with ispec. *Astronomy Astrophysics*, *569*, A111. https://doi.org/10.1051/0004-6361/201423945

Blanco-Cuaresma, S. (2019). Modern stellar spectroscopy caveats. *Monthly Notices of the Royal Astronomical Society*, *486*, 2075–2101. https://doi.org/10.1093/mnras/stz549

Bland-Hawthorn, J., & Gerhard, O. (2016). The galaxy in context: Structural, kinematic, and integrated properties. *Annual Review of Astronomy and Astrophysics*, *54*, 529–596. https://doi.org/10.1146/annurev-astro-081915-023441

Brown, A. M., Massey, R., Lacroix, T., Strigari, L. E., Fattahi, A., & Bœhm, C. (2019). The glow of annihilating dark matter in omega centauri. *arXiv:1907.08564 [astro-ph]*. https://arxiv.org/abs/1907.08564

Cayrel de Strobel, G., Soubiran, C., Friel, E. D., Ralite, N., & François, P. (1997). A catalogue of [fe/h] determinations: 1996 edition. *Astronomy and Astrophysics Supplement Series*, *124*, 299–305. https://doi.org/10.1051/aas:1997194

Cooper, A. P., Cole, S., Frenk, C. S., White, S. D. M., Helly, J., Benson, A. J., De Lucia, G., Helmi, A., Jenkins, A., Navarro, J. F., Springel, V., & Wang, J. (2010). Galactic stellar haloes in the cdm model. *Monthly Notices of the Royal Astronomical Society*, *406*, 744–766. https://doi.org/10.1111/j.1365-2966.2010.16740.x

Dekker, H., D'Odorico, S., Kaufer, A., Delabre, B., & Kotzlowski, H. (2000). Design, construction, and performance of uves, the echelle spectrograph for the ut2 kueyen telescope at the eso paranal observatory (M. Iye & A. F. M. Moorwood, Eds.). *Optical and IR Telescope Instrumentation and Detectors*. https://doi.org/10.1117/12.395512

ESA, M. R. (2022). Gaia reveals that most milky way companion galaxies are newcomers to our corner of space. *www.esa.int*. https://www.esa.int/Science_Exploration/Space_Science/Gaia/Gaia_reveals_that_most_Milky_Way_companion_galaxies_are_newcomers_to_our_corner_of_space

Gaia, C. (2020). Vizier online data catalog: Gaia edr3 (gaia collaboration, 2020). *VizieR Online Data Catalog*, I/350. https://ui.adsabs.harvard.edu/abs/2020yCat.1350....0G/abstract

Gebek, A., & Matthee, J. (2022). On the variation in stellar -enhancements of star-forming galaxies in the eagle simulation. *The Astrophysical Journal*, *924*, 73. https://doi.org/10.3847/1538-4357/ac350b

Gray, R. (2021). Documentation for spectrum v2.76. Retrieved June 29, 2022, from https://www.appstate.edu/~grayro/spectrum/spectrum276.pdf

Gustafsson, B., Edvardsson, B., Eriksson, K., Jørgensen, U. G., Nordlund, Å., & Plez, B. (2008). A grid of marcs model atmospheres for late-type stars. *Astronomy Astrophysics*, *486*, 951–970. https://doi.org/10.1051/0004-6361:200809724

Hansen, C. (2022). Heavy elements they came out of the blue. Retrieved June 25, 2022, from https://arxiv.org/pdf/2203.07396.pdf

Hawkins, K., Jofré, P., Masseron, T., & Gilmore, G. (2015). Using chemical tagging to redefine the interface of the galactic disc and halo. *Monthly Notices of the Royal Astronomical Society*, *453*, 758–774. https://doi.org/10.1093/mnras/stv1586

Helmi, A., Babusiaux, C., Koppelman, H. H., Massari, D., Veljanoski, J., & Brown, A. G. A. (2018). The merger that led to the formation of the milky way's inner stellar halo and thick disk. *Nature*, *563*, 85–88. https://doi.org/10.1038/s41586-018-0625-x

Hinkel, N. R., Timmes, F., Young, P. A., Pagano, M. D., & Turnbull, M. C. (2014). Stellar abundances in the solar neighborhood: The hypatia catalog. *The Astronomical Journal*, *148*, 54. https://doi.org/10.1088/0004-6256/148/3/54

Hinkle, K., Pacific, A. S. O. T., & Al, E. (2000). *Visible and near infrared atlas of the arcturus spectrum 3727-9300 å*. Astronomical Society Of The Pacific.

Holmbeck, E. M., Beers, T. C., Roederer, I. U., Placco, V. M., Hansen, T. T., Sakari, C. M., Sneden, C., Liu, C., Lee, Y. S., Cowan, J. J., & Frebel, A. (2018). The r -process alliance: 2mass j09544277+5246414, the most actinide-enhanced r -ii star known. *The Astrophysical Journal*, *859*, L24. https://doi.org/10.3847/2041-8213/aac722

Ibata, R., Bellazzini, M., Malhan, K., Martin, N., & Bianchini, P. (2019). Identification of the long stellar stream of the prototypical massive globular cluster ω centauri. *arXiv:1902.09544 [astro-ph]*. Retrieved June 27, 2022, from https://arxiv.org/abs/1902.09544

Leblanc, F. (2010). *An introduction to stellar astrophysics*. Wiley.

Massari, D., Koppelman, H. H., & Helmi, A. (2019). Origin of the system of globular clusters in the milky way. *Astronomy Astrophysics*, *630*, L4. https://doi.org/10.1051/0004-6361/201936135

McWilliam, A. (1997). Abundance ratios and galactic chemical evolution. *Annual Review of Astronomy and Astrophysics*, *35*, 503–556. https://doi.org/10.1146/annurev.astro.35.1.503

Nissen, & Schuster, W. (2010). Evidence from stellar abundance ratios and kinematics. *AA*, *511*, 10. https://doi.org/10.1051/0004-6361/200913877

Nissen, & Schuster, W. J. (2012). Two distinct halo populations in the solar neighborhood. *Astronomy Astrophysics*, *543*, A28. https://doi.org/10.1051/0004-6361/201219342

Roederer, I. U., Sakari, C. M., Placco, V. M., Beers, T. C., Ezzeddine, R., Frebel, A., & Hansen, T. T. (2018). Ther-process alliance: A comprehensive abundance analysis of hd 222925, a metal-poor star with an extremer-process enhancement of [eu/h] = 0.14. *The Astrophysical Journal*, *865*, 129. https://doi.org/10.3847/1538-4357/aadd92

Schuler, S. C., Andrews, J. J., Clanzy, V. R., Mourabit, M., Chanamé, J., & Agüeros, M. A. (2021). Combining astrometry and elemental abundances: The case of the candidate pre-

gaia halo moving groups g03-37, g18-39, and g21-22 [*]. *The Astronomical Journal*, *162*, 109. https://doi.org/10.3847/1538-3881/ac10c6

Schuster, W. J., Moreno, E., & Fernández-Trincado, J. G. (2018). Resonant trapping of the moving groups g18-39 and g21-22 in the galactic halo. *Proceedings of the International Astronomical Union*, *14*, 134–138. https://doi.org/10.1017/s174392131800683x

Schuster, W. J., Moreno, E., Nissen, P. E., & Pichardo, B. (2012). Two distinct halo populations in the solar neighborhood. *Astronomy Astrophysics*, *538*, A21. https://doi.org/10.1051/0004-6361/201118035

Silva, J., Schuster, W., & Contreras, M. (2012). Uvby- photometry and kinematics of metal-poor stars: A search for moving groups in the galactic stellar halo physical studies of planetary nebulae view project uvby - photometry and kinematics of metal-poor stars: A search for moving groups in the galactic stellar halo. *Revista Mexicana de Astronomía y Astrofísica*, *48*, 109–136.

SIMBAD (Ed.). (n.d.). G18-39. *simbad.u-strasbg.fr*. Retrieved June 25, 2022, from https://simbad.u-strasbg.fr/simbad/sim-id?Ident=g18-39&NbIdent=1&Radius=2&Radius.unit=arcmin&submit=submit+id

Sparke, L. S., & Gallagher, J. S. (2010). *Galaxies in the universe : An introduction*. Cambridge Univ. Press.

Stahler, S. W., & Palla, F. (2004). *The formation of stars*. Wiley-Vch.

Sumiyoshi, K. (2002). R-process nucleosynthesis in supernova explosions. *Progress of Theoretical Physics Supplement*, *146*, 258–267. https://doi.org/10.1143/ptps.146.258

Tolstoy, E., Hill, V., & Tosi, M. (2009). Star-formation histories, abundances, and kinematics of dwarf galaxies in the local group. *Annual Review of Astronomy and Astrophysics*, *47*, 371–425. https://doi.org/10.1146/annurev-astro-082708-101650

Wang, H.-F., Yang, Y.-B., Hammer, F., & Wang, J.-L. (2022). Reconstructing the whole 6d properties of the sagittarius stream with n-body simulation. *arXiv:2204.08542 [astro-ph]*. Retrieved June 27, 2022, from https://arxiv.org/abs/2204.08542

Yamazaki, Y., Kajino, T., Mathews, G. J., Tang, X., Shi, J., & Famiano, M. A. (2021). Contribution of collapsars, supernovae, and neutron star mergers to the evolution of r-process elements in the galaxy. *arXiv:2102.05891 [astro-ph]*. Retrieved June 27, 2022, from https://arxiv.org/abs/2102.05891

Yang, Y., Hammer, F., Jiao, Y., & Pawlowski, M. S. (2022). An extended stellar halo discovered in the fornax dwarf spheroidal using gaia edr3. *Monthly Notices of the Royal Astronomical Society*, *512*, 4171–4184. https://doi.org/10.1093/mnras/stac644

Yao, Y., & Wang, Q. D. (2007). The galactic central diffuse x-ray enhancement: A differential absorption/emission analysis. *The Astrophysical Journal*, *666*, 242–246. https://doi.org/10.1086/519825

Yushchenko, A., Gopka, V., Goriely, S., Musaev, F., Shavrina, A., Kim, C., Woon Kang, Y., Kuznietsova, J., & Yushchenko, V. (2005). Thorium-rich halo star hd221170: Further evidence against the universality of the r-process. *Astronomy Astrophysics*, *430*, 255–262. https://doi.org/10.1051/0004-6361:20041540

8 Appendix

For Kapteyn users: the directory

`/net/virgo01/data/users/angrilli/g18-39`

is open to anyone who would like to retrieve the data that I have been working with. It contains a directory called "Benchmarks", containing the benchmark stars around which we developed our method. It also contains three txt files: one contains raw data as retrieved from UVES observations. If the errors are missing one can add them using S/N = 480. There is a file named "g18-39_norm.txt" which contains the normalised spectrum, where the continuum goes through the noise, but the synthesis has not been done yet. Then, there is a file named "g18-39_synth.txt" which is my best estimate at normalising the spectrum via the synthesis.

For non Kapteyn users: you can contact me via email for the data.